ALMA Memo. No. 365

Atmospheric Phase Stability at Chajnantor and Pampa la Bola

Bryan J. Butler and Simon J. E. Radford
National Radio Astronomy Observatory

Seiichi Sakamoto
National Astronomical Observatory of Japan

Kotaro Kohno
Nobeyama Radio Observatory

2001-Jun-06

Introduction

Atmospheric phase stability has been measured at Chajnantor (e.g., Radford & Holdaway 1998) and Pampa la Bola (e.g., Ishiguro 1998) for many years now with Site Test Interferometers (STIs - see Ishiguro *et al.* 1989; Radford *et al.* 1996). A preliminary analysis of these data showed Chajnantor had smaller phase fluctuations than Pampa la Bola (Holdaway *et al.* 1997), but only 6 weeks worth of data were included in that analysis. Given the more extensive data set available now, it seems appropriate to make a more complete comparison.

Data

Although they differ in some details both interferometers share the same design. They observe an unmodulated 11.198 GHz beacon broadcast by a geostationary Intelsat satellite (IS-603). Each instrument has two antennae at the ends of a 300 m, east-west baseline. The satellite position is 35 deg above the horizon and 68 deg east from north. The relevant measured quantity in this study is the relative phase between the two antennas. Because this is a relative (differential) quantity, calibration differences between the two instruments should not affect our analysis or conclusions.

The raw phases measured by the STIs at each site are recorded at roughly 1 second intervals. These phases are then grouped into 10 minute intervals and a temporal phase structure function is calculated. From the raw phases and the structure function, three quantities are calculated for each 10 min interval: the rms amplitude of the phase fluctuations, $\phi_{\rm rms}$, the corner time, $t_{\rm corner}$, and the exponent of the power law at short times, α. The rms phase fluctuations, $\phi_{\rm rms}$, are related to the "saturation phase" - the rms phase fluctuations at long times. The data reduction technique is described in more detail in Butler & Desai (1999).

One detail deserves some discussion. The electronic noise introduced by the instrument itself complicates the analysis of the STI data. Holdaway *et al.* (1995) found a white electronic noise term with an 0.18° rms amplitude provided the best fit to the data taken at the Chajnantor STI. This corresponds to 0.25° in the square root structure function. Butler & Desai (1999) completely ignored the electronic noise term, since it was never apparent in the STI data taken at the VLA (similar to the Mauna Kea data discussed by Holdaway *et al.* [1995]). We have analyzed all the overlapping (see below) data from Chajnantor and Pampa la Bola and find the best estimates for the rms amplitudes of the electronic noise terms are 0.14° and 0.26° for Chajnantor and Pampa la Bola, respectively. We use these values in the present analysis.

Data from both sites are available for 1996 July – 1999 March. Nearly concurrent data were selected where the center times of the 10 min intervals for both sites fell within 5 min. Distributions were then calculated for these concurrent data. In all, 24887 concurrent 10 min intervals were included in the study. Although common coverage (Figure 1) is far from complete over the entire study period, it should be sufficient for broad comparisons. Moreover, seasonal coverage (Figure 2) is nearly complete, except mid January to mid February.

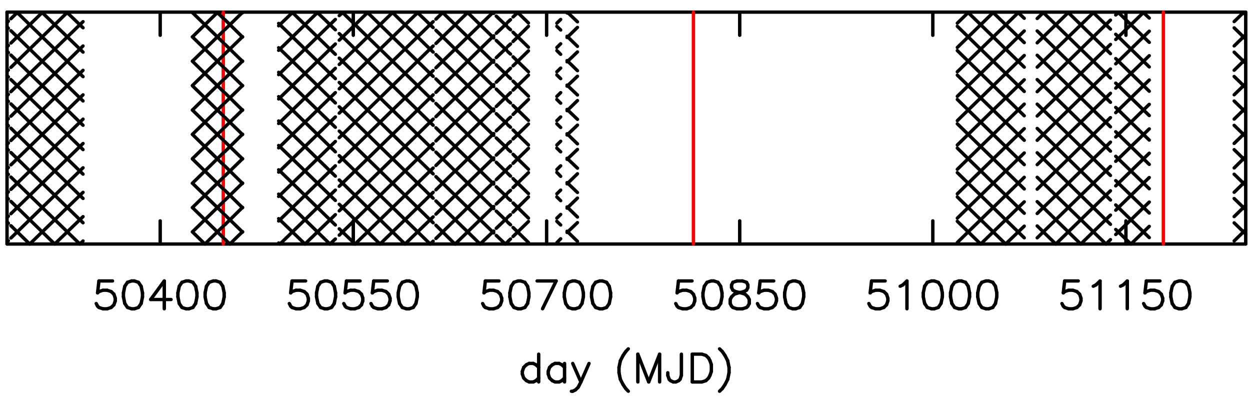

Figure 1: Common coverage for the STI instruments at Pampa la Bola and Chajnantor during the period 1996 July – 1999 March. Hatched areas are times when common data exists. The vertical red lines are the markers for January 1 of 1997, 1998, and 1999.

Results

Overall Results

The cumulative distributions of $\phi_{\rm rms}$ measured at the two sites are shown in Figure 3.

Table 1 summarizes the $10^{\rm th}$, $25^{\rm th}$, $50^{\rm th}$, and $75^{\rm th}$ percentiles for the distributions of the three main quantities for the two sites. Note that the distributions are calculated independently for each quantity. Also included in that table is the number for ϕ_{10s}, the magnitude of the rms phase fluctuations at 10 second timescales. This is a number that will be of interest later.

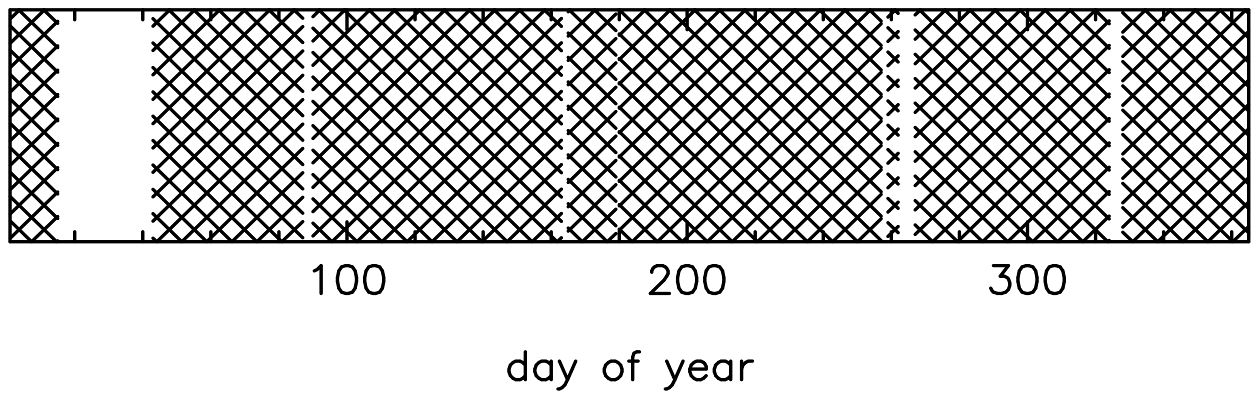

Figure 2: Common coverage for the STI instruments at Pampa la Bola and Chajnantor plotted as a function of day of year. Hatched areas are days when common data exists.

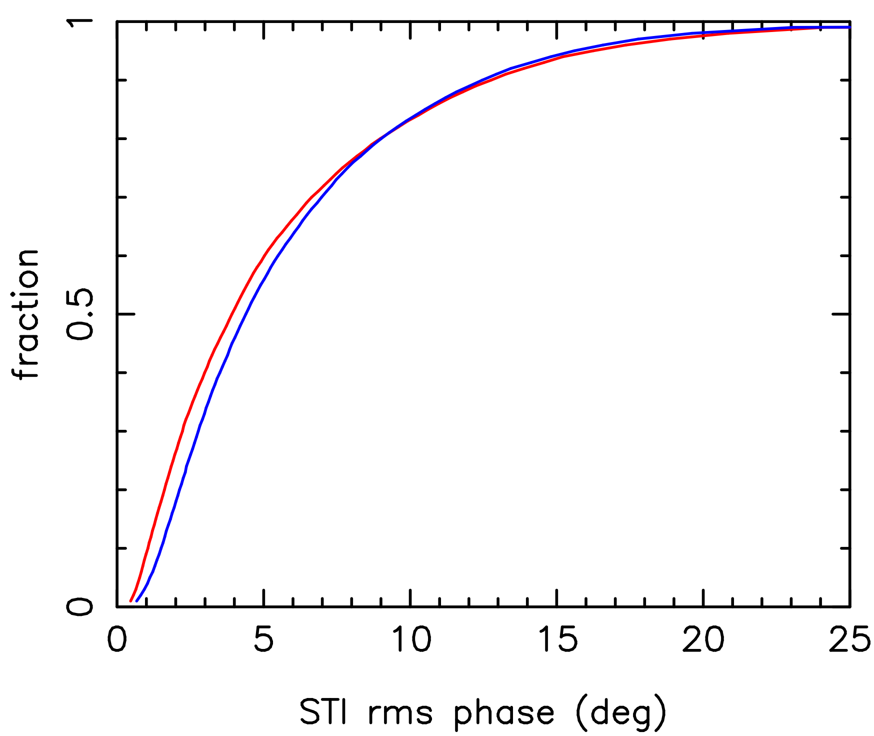

Figure 3: Cumulative distributions of ϕ_{rms} at Chajnantor (red line) and Pampa la Bola (blue line). The data were taken at 11.198 GHz and 35° elevation on a 300 m baseline.

Table 1: Measured STI quantities for Chajnantor and Pampa la Bola.

	Chajnantor				Pampa la Bola			
percentile	$\phi_{\rm rms}$ (deg)	t_{corner} (s)	α	ϕ_{10s} (deg)	$\phi_{\rm rms}$ (deg)	t_{corner} (s)	α	ϕ_{10s} (deg)
10	1.05	10.71	0.42	0.56	1.50	11.96	0.500	0.71
25	1.91	14.75	0.55	0.94	2.44	15.82	0.580	1.16
50	3.92	21.85	0.63	1.77	4.39	23.83	0.640	2.00
75	7.69	32.93	0.69	3.17	7.86	35.94	0.700	3.30

Seasonal Variation

The monthly 10$^{\rm th}$ and 50$^{\rm th}$ percentiles of $\phi_{\rm rms}$ measured at both sites (Figure 4) show the expected seasonal variation. In general, the phase stability is worse in summer than in winter. June stands out as an exception. The common data were collected in 1997 June, however, when particularly bad conditions existed, perhaps attributable to the El Niño Southern Oscillation. Data from Chajnantor for other years do not show increased phase fluctuations in June.

During summer (October – February), the phase stability at both sites is similar, perhaps reflecting the slightly more adverse effect of the Altiplanic winter on the Chajnantor site. For all other months, the phase stability at Chajnantor is significantly less than that at Pampa la Bola, at both the median and the 10$^{\rm th}$ percentile.

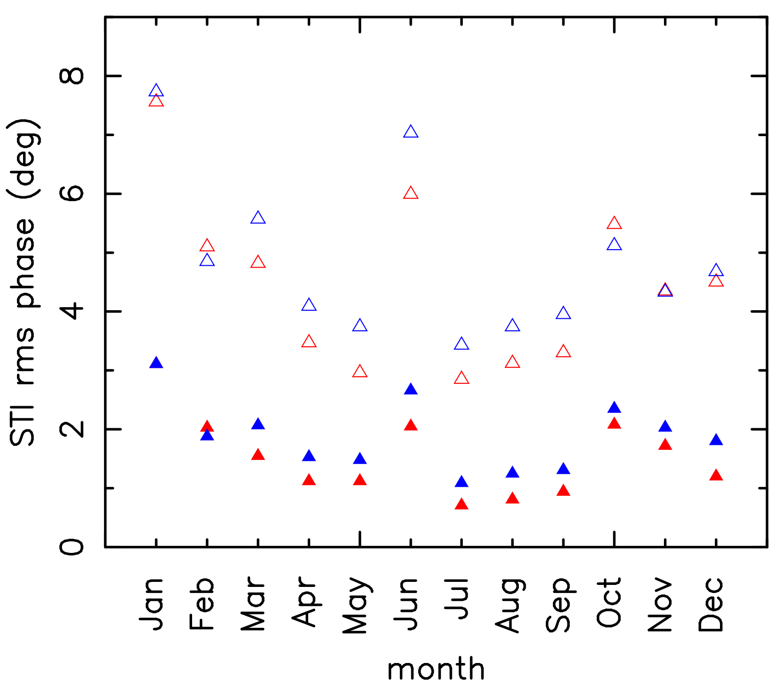

Figure 4: 10$^{\rm th}$ (filled triangles) and 50$^{\rm th}$ (open triangles) percentiles of $\phi_{\rm rms}$ plotted vs. month at Chajnantor (red symbols) and Pampa la Bola (blue symbols). The data were taken at 11.198 GHz and 35° elevation on a 300 m baseline.

Diurnal Variation

The hourly 10th and 50th percentiles of $\phi_{\rm rms}$ measured at both sites (Figure 5) show a clear day/night variation. Note that the daily excursion at Pampa la Bola is less than at Chajnantor. Throughout most of the day, the phase stability at Chajnantor is better than at Pampa la Bola, at both the median and the 10th percentile.

During the period from mid-morning to mid-afternoon (roughly UT 15h to 21h), however, the phase stability at Pampa la Bola is better than at Chajnantor. This midday result is contrary to a widely accepted model of the origin of phase fluctuations at these locations. In this accepted model, wind flows from the west over Cerros Chajnantor and Toco and becomes turbulent downstream. This model then predicts that phase stability should be better at Chajnantor than at Pampa la Bola during the windiest conditions, which generally occur during the afternoon. In fact, this is not observed. Note that the accepted model also has difficulty explaining the seasonal variation, since winds are generally stronger in the winter than the summer.

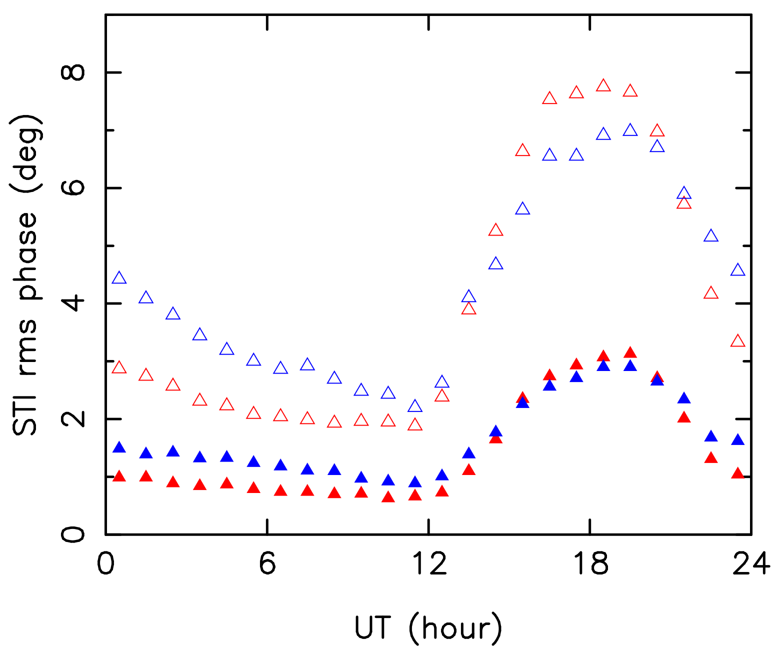

Figure 5: 10th (filled triangles) and 50th (open triangles) percentiles of $\phi_{\rm rms}$ plotted vs. hour at Chajnantor (red symbols) and Pampa la Bola (blue symbols). The data were taken at 11.198 GHz and 35° elevation on a 300 m baseline. Local solar time of day is UT - 4h31m.

Effect on Observing Time

Phase fluctuations will cause an effective degradation in SNR which can only be recovered by increasing the observing time. Given atmospheric phase fluctuations of a magnitude σ_ϕ at frequency ν, the atmospheric coherence $R(\nu)$ is given by (see e.g., Thompson *et al.* 1991, pages 429-432):

$$R(\nu) = e^{-\sigma_\phi^2(\nu)/2} \quad . \tag{1}$$

This is the reduction in visibility SNR due to the atmospheric phase fluctuations. The phase fluctuations at frequencies in the spectral windows between the resonant line absorptions, where the atmosphere is mostly non-dispersive (and where ALMA will be observing the bulk of the time), can be determined by scaling the measured STI phase fluctuations:

$$\sigma_\phi(\nu) = \sigma_\phi(11.198)\ \frac{\nu_{\rm GHz}}{11.198} \quad , \tag{2}$$

where $\nu_{\rm GHz}$ is the frequency in GHz. Note that in regions where the phase is dispersive (near window edges, e.g.), this linear relation breaks down, and the problem of scaling phase from a lower to a higher frequency is much more difficult (M. Holdaway, in preparation). Now, the proper value to use for $\sigma_\phi(11.198)$ is the value that occurs for the "calibration timescale". That timescale is the shortest of either: the source-cal-source switching time; the corner time $t_{\rm corner}$; the WVR calibration time; or the self-calibration time. Although initial experiments are encouraging, WVR is not yet in routine operational use anywhere. Our current expectation is that the calibration switching cycle time might be as fast as 10 sec (at least for fast switching observations). If we have a source that is weak enough that it cannot be self-calibrated on timescales shorter than 10 sec, then that time (10 sec) is the applicable timescale. We can substitute values of the measured phase fluctuations at 10 sec lag (take the calculated value of the phase structure function at 10 sec lag, divide by 2, and take the square root - this gives the phase rms at 10 sec lag) for $\sigma_\phi(11.198)$. Given relative SNR at Pampa la Bola and Chajnantor, then the ratio of observing time is given by:

$$t' = \frac{t_{\rm obs}({\rm bola})}{t_{\rm obs}({\rm chaj})} = \left(\frac{R_{\rm chaj}(\nu)}{R_{\rm bola}(\nu)}\right)^2 \quad . \tag{3}$$

So, if $t' > 1$, then it takes more observing time at Pampa la Bola to achieve the same SNR as at Chajnantor. Assuming an observing frequency of 345 GHz, then the relative observing times shown in Table 2 result, as a function of time of day. Note that this table is calculated for the $10^{\rm th}$ percentile measured STI phase (at 10 second lag). The ratio can be as large as a factor of 2. Note that at the times when the phase stability is better at Pampa la Bola than at Chajnantor (roughly UT 15h to 21h), the phase fluctuations are > 1 radian at both locations.

Summary

The median rms phase stability at Chajnantor is $\sim$ 12% better than at Pampa la Bola, averaged over all times. This is similar to the result of a preliminary study by Holdaway *et al.* (1997). The $10^{\rm th}$ percentile rms phase stability at Chajnantor is $\sim$ 43% better than at Pampa la Bola. During most of the day, the phase stability at Chajnantor is better than at Pampa la Bola. There is a period from around UT 15h to UT 21h (mid-morning to mid-afternoon), during which the phase stability is better at Pampa la Bola. This cannot be

Table 2: Ratio of Observing Time vs. hour between Pampa la Bola and Chajnantor at 345 GHz. Values of phase are the 10th percentile for 10 second timescales, on a 300 m baseline, at 35° elevation, and shown for both 11.198 GHz (the measured frequency) and 345 GHz (scaled from the measurement).

	Chajnantor			Pampa la Bola			
hour	$\phi_{10s}(11.198)$ (deg)	$\phi_{10s}(345)$ (deg)	$R(345)$	$\phi_{10s}(11.198)$ (deg)	$\phi_{10s}(345)$ (deg)	$R(345)$	t'
0-1	1.52	46.8	0.72	2.22	68.4	0.49	2.13
1-2	1.43	44.0	0.74	2.03	62.5	0.55	1.82
2-3	1.44	44.4	0.74	1.88	57.9	0.60	1.53
3-4	1.29	39.7	0.79	1.70	52.4	0.66	1.43
4-5	1.25	38.5	0.80	1.60	49.3	0.69	1.33
5-6	1.13	34.8	0.83	1.47	45.3	0.73	1.29
6-7	1.07	33.0	0.85	1.39	42.8	0.76	1.26
7-8	1.07	33.0	0.85	1.38	42.5	0.76	1.25
8-9	1.04	32.0	0.86	1.33	41.0	0.77	1.22
9-10	0.99	30.5	0.87	1.18	36.3	0.82	1.13
10-11	0.99	30.5	0.87	1.17	36.0	0.82	1.12
11-12	1.06	32.7	0.85	1.09	33.6	0.84	1.02
12-13	1.23	37.9	0.80	1.28	39.4	0.79	1.04
13-14	1.64	50.5	0.68	1.65	50.8	0.67	1.01
14-15	2.09	64.4	0.53	1.96	60.4	0.57	0.86
15-16	2.63	81.0	0.37	2.33	71.8	0.46	0.65
16-17	2.97	91.5	0.28	2.66	81.9	0.36	0.60
17-18	3.15	97.0	0.24	2.87	88.4	0.30	0.61
18-19	3.27	100.7	0.21	3.03	93.3	0.27	0.65
19-20	3.32	102.3	0.20	3.10	95.5	0.25	0.66
20-21	3.22	99.2	0.22	3.10	95.5	0.25	0.80
21-22	2.78	85.6	0.33	2.89	89.0	0.30	1.20
22-23	2.14	65.9	0.52	2.49	76.7	0.41	1.60
23-24	1.70	52.4	0.66	2.26	69.6	0.48	1.90
all	1.77	54.5	0.64	2.00	61.6	0.56	1.28

explained by wind flow over Cerros Chajnantor and Toco generating downstream turbulence. If we are unable to correct for the phase fluctuations on timescales faster than 10 seconds, then the observing time required to reach the same SNR can be half as long or less at Chajnantor as compared to Pampa la Bola.

References

Butler, B., & K. Desai, Phase Fluctuations at the VLA Derived From One Year of Site Testing Interferometer Data, VLA Test Memo. No. 222, 1999

Holdaway, M.A., S. Matsushita, & M. Saito, Preliminary Phase Stability Comparison of the Chajnantor and Pampa la Bola sites, MMA Memo. No. 176, 1997

Holdaway, M.A., S.J.E. Radford, F.N. Owen, & S.M. Foster, Data Processing for Site Test Interferometers, MMA Memo. No. 129, 1995

Ishiguro, M., Japanese Large Millimeter and Submillimeter Array, *Proc. SPIE, 3357*, 244-253, 1998

Ishiguro, M., T. Kanzawa, & T. Kasuga, Monitoring of Atmospheric Phase Fluctuations Using Geostationary Satellite Signals, in *Radio Astronomical Seeing*, ed. J.E. Baldwin & W. Shouguan, 1989

Radford, S.J.E., & M.A. Holdaway, Atmospheric conditions at a site for submillimeter wavelength astronomy, *Proc. SPIE, 3357*, 486-494, 1998

Radford, S.J.E., G. Reiland, & B. Shillue, Site Test Interferometer, *PASP, 108*, 441–445, 1996

Thompson, A.R., J.M. Moran, and G.W. Swenson, Jr., *Interferometry and Synthesis in Radio Astronomy*, 2nd ed., 1991